Investigation of magnetic fluctuations in $Tb_2Sn_2O_7$ ordered spin ice by high-resolution energy-resolved neutron scattering

I. Mirebeau,[1] H. Mutka,[2] P. Bonville,[3] A. Apetrei,[1] and A. Forget[3]
[1]*Laboratoire Léon Brillouin, CEA-CNRS, CE-Saclay, 9191 Gif-sur-Yvette, France*
[2]*Institut Laüe Langevin, 6 rue Jules Horowitz, BP 156X, 38042 Grenoble, France*
[3]*Service de Physique de l'Etat Condensé, CEA-CNRS, CE-Saclay, 91191 Gif-sur-Yvette, France*
(Received 4 June 2008; revised manuscript received 17 October 2008; published 17 November 2008)

We have studied magnetically frustrated $Tb_2Sn_2O_7$ by neutron diffraction and high-resolution energy-resolved neutron scattering. At 0.1 K, we observed short-range magnetic correlations with a typical scale of 4 Å, close to the near-neighbor distance between Tb^{3+} ions. This short-range order coexists with ferromagnetic correlations and long-range spin ice order at the scales of 18 and 190 Å, respectively. Spin dynamics was investigated at a time scale down to 10^{-9} s by energy-resolved experiments on a backscattering spectrometer. We observed a freezing of the spin dynamics for all length scales with a strong slowing down of the spin fluctuations when long-range order settles in. We discuss the spin fluctuations remaining in the ground state, in comparison with previous data obtained by muon spectroscopy.

DOI: 10.1103/PhysRevB.78.174416 PACS number(s): 75.25.+z, 71.27.+a

I. INTRODUCTION

Geometrical frustration is expected to favor the onset of unusual types of order such as spin liquid and spin ices, showing a large degeneracy of the magnetic ground state. In spin ices, it leads to nonzero ground-state entropy akin to that of real ice,[1] peculiar freezing dynamics,[2] and short-range magnetic orders.[3,4] Application of a magnetic field lifts the ice rule degeneracy,[5] yielding to excitations which span the entire system,[6] or are akin to magnetic monopoles,[7] depending on the orientation of the field with respect to the anisotropy axis.

Canonical spin ices are observed in pyrochlores $R_2Ti_2O_7$ (R=Dy or Ho), where the rare-earth moments occupy a lattice of corner sharing tetrahedra. The stabilization of the spin ice ground state is related to the strong anisotropy of the Dy^{3+} or Ho^{3+} ions, whose moments are constrained to lie along the ⟨111⟩ local axes connecting the center of each tetrahedron to the summits.

The Tb pyrochlores offer a more complex but even richer behavior due to the smaller anisotropy of the Tb^{3+} ion, and to the fact that superexchange and dipolar interactions between near-neighbor Tb^{3+} ions nearly compensate. $Tb_2Sn_2O_7$ is an intriguing example of an ordered spin ice.[8] Contrarily to classical spin ices which do not order at large scale, here the four tetrahedra of the unit cell are identical, yielding magnetic Bragg peaks and long-range order (LRO), at a length scale which increases with decreasing temperature T and reaches about 190 Å at T=0. The onset of this magnetic order is observed at T_I=1.3(1) K. An upturn of the correlation length and magnetic moment, together with a peak in the specific heat, occurs at T_C=0.87(2) K.

Magnetic fluctuations play a prominent role in the ordered spin state of $Tb_2Sn_2O_7$. They were first evidenced by the reduction of the ordered moment as measured using the hyperfine Schottky anomaly of the specific heat and compared with its value from neutron diffraction.[8] Then they were directly observed using μSR.[9,10] Surprisingly, no direct evidence of a static component appears in the local field probed by zero field μSR in spite of the presence of the magnetic order. The fluctuations of the local field occur at a time scale estimated either to be 8×10^{-11} s or to be 5×10^{-9} s, depending mostly on the value assumed for the local field.[9,10] Under applied field, damped oscillations in the muon polarization and a thermal hysteresis in the longitudinal relaxation rate show the presence of locally ordered configurations frozen at the time scale of the muon probe.[10]

Very recently, several inelastic neutron-scattering measurements were performed to study the magnetic fluctuations in $Tb_2Sn_2O_7$. Crystal field excitations[11] were measured down to 1.4 K and compared to those in $Tb_2Ti_2O_7$, which remains spin liquid down to about 50 mK. It was shown that the wave functions describing the ground and first-excited states of the Tb^{3+} ion were exchanged in the two compounds.[11] However, these differences in the local states of the Tb^{3+} ion cannot explain the different cooperative ground states in the Ti and Sn compounds within the frame of current theories.

Neutron spin-echo (NSE) measurements[12] were performed in $Tb_2Sn_2O_7$ for a moment transfer Q=0.08 $Å^{-1}$ outside the Bragg-peak positions, probing the dynamics of the ferromagnetic correlations. They clearly observed some spin dynamics down to 0.8 K but failed to detect any below. Finally, the magnetic cross section was measured by polarized neutrons.[13] The spin dynamics was deduced from the comparison between diffraction measurements (integrating the magnetic signal over all energies up to 3 meV) and elastic scattering with a coarse energy resolution (integration over an energy window of ±0.15 meV). At 0.04 K, the authors conclude to the presence of static Bragg peaks, together with a liquidlike structure factor arising from spins moving faster than 0.04 THz.

Here we have investigated the spin correlations and dynamics in $Tb_2Sn_2O_7$ by combining neutron-diffraction and energy-resolved neutron-scattering measurements with a very high energy resolution of 0.5 μeV at half width at half maximum (HWHM), probing time scales up to 1.3×10^{-9} s. Both measurements were performed in the temperature range of 0.1–1.4 K. The Q and T dependences of the

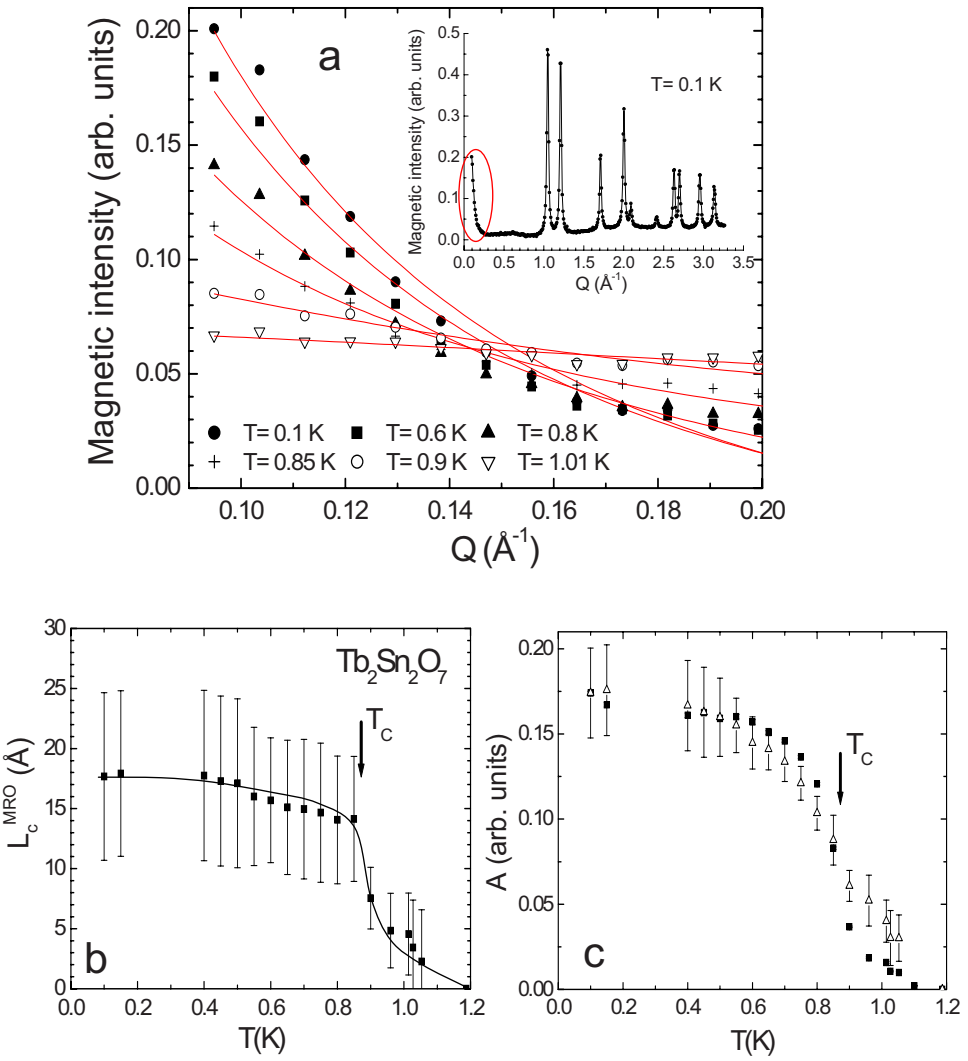

FIG. 1. (Color online) (a) Magnetic intensity measured $Tb_2Sn_2O_7$ by neutron diffraction at small angles versus the moment transfer Q for several temperatures. A spectrum above 1.2 K was subtracted. Solid lines are Lorentzian fits (see text). In the inset, the total diffraction pattern at 0.1 K, showing the small-angle intensity together with the magnetic Bragg peaks. (b) Medium correlation length $L_C^{MRO}=1/\kappa$ (full squares) versus temperature T. The solid line is a guide to the eye. (c) Norm A of the Lorentzian (open triangles) and intensity of the magnetic Bragg peaks (full squares) versus temperature.

magnetic scattering were analyzed quantitatively, considering not only the Bragg scattering but also the medium and short-range correlations. Diffraction data measured at 0.1 K show the coexistence of several length scales, corresponding to first neighbors (~4 Å), medium (18 Å), and long-range (190 Å) correlations. The spin dynamics was investigated in different Q ranges where either short or long length scales are dominant. When T decreases, we observe a freezing of the spin dynamics for all length scales with a stronger effect in the region of the transition. Some spin fluctuations persist down to the lowest temperature of 0.1 K. We discuss these results with respect to the fluctuations in the ground state in $Tb_2Sn_2O_7$.

II. NEUTRON DIFFRACTION

Neutron-diffraction measurements were performed on the D1B spectrometer at the Institut Laüe Langevin (ILL) with an incident neutron wavelength of 2.52 Å. The magnetic long-range order was already studied in Ref. 8 from the same data. The magnetic cross section was isolated by subtracting a spectrum measured at 1.2 K. The magnetic diffraction pattern at 0.1 K [inset of Fig. 1(a)] shows an intense small-angle neutron-scattering (SANS) signal for $Q<0.2$ Å^{-1}, arising from ferromagnetic correlations. The SANS signal [Fig. 1(a)] strongly increases with decreasing T and flattens in the range of the transition. It was fitted by a Lorentzian function $I(Q)=\frac{A}{\pi}\frac{\kappa}{\kappa^2+Q^2}$. Good fits are obtained down to about 0.6 K but the fit quality decreases below. The fit however allows one to estimate the medium correlation length $L_C^{MRO}=1/\kappa$ [Fig. 1(b)] versus temperature in the ordered region. With decreasing temperature, L_C^{MRO} increases from values close to the near-neighbor distance between Tb^{3+} moments ($d=3.686$ Å) to about 18(6) Å below 0.8 K. This value is about ten times smaller than that deduced from the width of the magnetic Bragg peaks ($L_C=190$ Å as shown in Ref. 8) but its temperature dependence is quite similar. The parameter A increases with decreasing temperature. Its variation compares well with that of the LRO squared magnetic moment deduced from the Bragg-peak intensity although it is less sharp in the transition region [Fig. 1(c)].

The short-range order (SRO) yields a diffuse magnetic scattering which remains clearly visible at 0.1 K. This scattering was not analyzed in Ref. 8. Here we refined it as a magnetic structure, assuming that it has the same symmetry as the LRO but a much shorter correlation length. The relative contributions of the SRO and LRO are shown in Fig. 2.

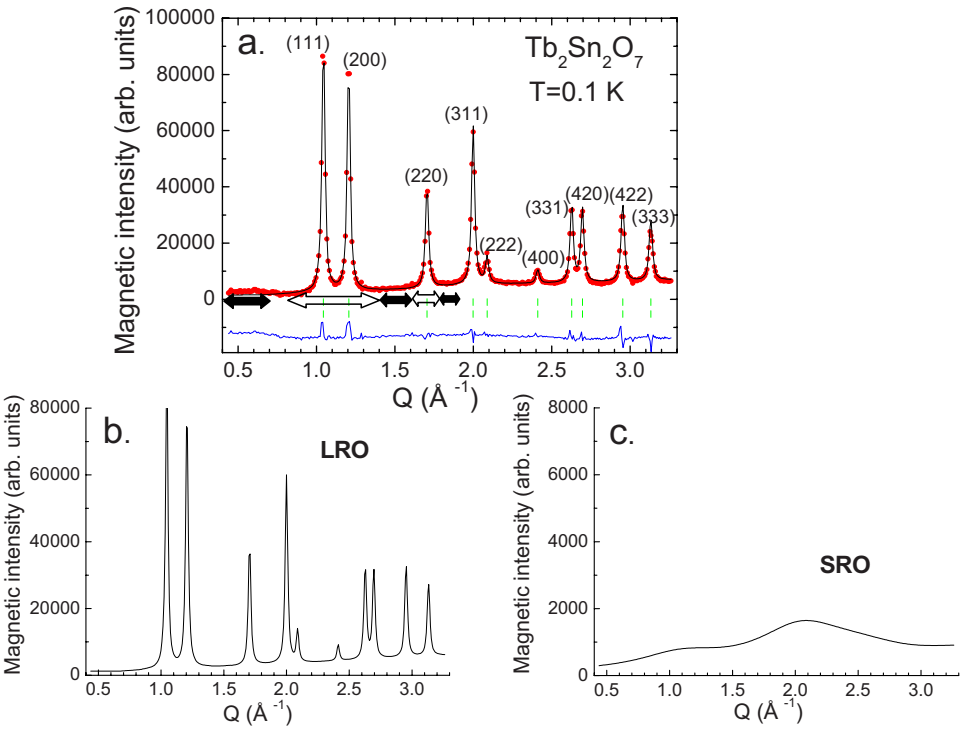

FIG. 2. (Color online) (a) Magnetic diffraction spectrum of $Tb_2Sn_2O_7$ versus the moment transfer Q at 0.1 K. A spectrum at 1.2 K was subtracted. The solid line is a refinement taking into account both LRO and SRO contributions. A linear background is also added. The arrows correspond to the Q bands selected in the time-resolved experiment. White arrows correspond to the Bragg Q bands, black arrows to the low, medium, and high Q bands. [(b) and (c)] Calculated LRO (SRO) contribution to the diffraction pattern.

From the fit, we obtain values of LRO and SRO moments of $5.8(1)\mu_B$ and $3.3(3)\mu_B$, respectively. The value of the LRO moment, ordered at the scale of 190 Å deduced from the width of the Bragg peaks, agree with the value previously determined as $5.9(1)\mu_B$. The SRO moment compares well with the value of about $3\mu_B$ obtained by calibration of the diffuse magnetic scattering measured with polarized neutrons.[13] This analysis shows that a large amount of the Tb^{3+} moments remains ordered at a very short length scale, estimated here to be 4(1) Å from the refinement, therefore comparable to the distance between first neighbor Tb^{3+} moments (3.686 Å). Assuming that both types of correlations contribute to the neutron intensity independently, we estimate the total ordered moment to $M=6.6(2)\mu_B/\mathrm{Tb}$. We notice that this value is exactly the value calculated for the total local moment within the crystal-field model (Fig. 15 of Ref. 11).

The above analysis shows the presence of three characteristic length scales for the spin correlations at low temperature, with values ranging from the first neighbor distance to length scales of about 18 cubic unit cells (the lattice constant $a=10.426$ Å). A distribution of length scales was previously inferred from an independent analysis of the profile peak shape.[12]

III. ENERGY RESOLVED NEUTRON SCATTERING

The analysis above motivates a study of the slow spin dynamics at different Q ranges, where either short or long length scales dominate. For this purpose we performed energy-resolved neutron-scattering measurements on the IN16 backscattering spectrometer of the ILL, with an incident neutron wavelength of 6.27 Å. This instrument offers a dynamic range of ± 15 μeV for the observation of fluctuations characterized by a quasielastic response. Due to the large angular acceptances of the backscattering method, the wave-vector transfer resolution is rather relaxed, anyhow sufficient in discriminating regions of interest with or without contributions from the Bragg peaks associated with the long-range ordering process. Optionally one can switch off the energy-transfer analysis to follow only the elastic response within the resolution window of 1 μeV at full width at half maximum (FWHM). Accordingly one can obtain a temperature scan of the elastic contribution over the whole Q range and compare intensity in specific Q bands to the temperature variation observed for the Bragg peaks in the diffraction experiment.

The sample was packed in a 1-mm-thick flat can in order to minimize the sample absorption. The transmission was evaluated to 0.9. The counting time was 12 h for each temperature. A vanadium sample of the same shape was measured to calibrate the angle dependent detection efficiency and to determine the energy resolution.

The spectra were corrected for background and absorption using spectra of the empty sample holder measured in the same conditions, taking into account the specific corrections due to the backscattering geometry.[14] Temperature scan of the elastic resolved scattering was taken in the range of $0.1\ \mathrm{K} \leq T < 1.4\ \mathrm{K}$. The quasielastic spectra were recorded in a range of $0.1\ \text{Å}^{-1} < Q < 1.9\ \text{Å}^{-1}$. They were grouped into five Q bands: three bands out of the Bragg peaks and two at the Bragg-peak positions. The Q bands outside the Bragg peaks are, respectively, called the low Q band ($Q=0.55\pm0.15$ Å^{-1}), the medium Q band ($Q=1.5\pm0.1$ Å^{-1}), and the high Q band ($Q=1.85\pm0.05$ Å^{-1}). The Q bands at the Bragg-peak positions are, respectively, $Q_{111+200}=1.1\pm0.3$ Å^{-1} and $Q_{220}=1.7\pm0.1$ Å^{-1}, the first for the 111 and 200 together (not well resolved individually) and the second for 220 contribution. The 311 Bragg peak is out of

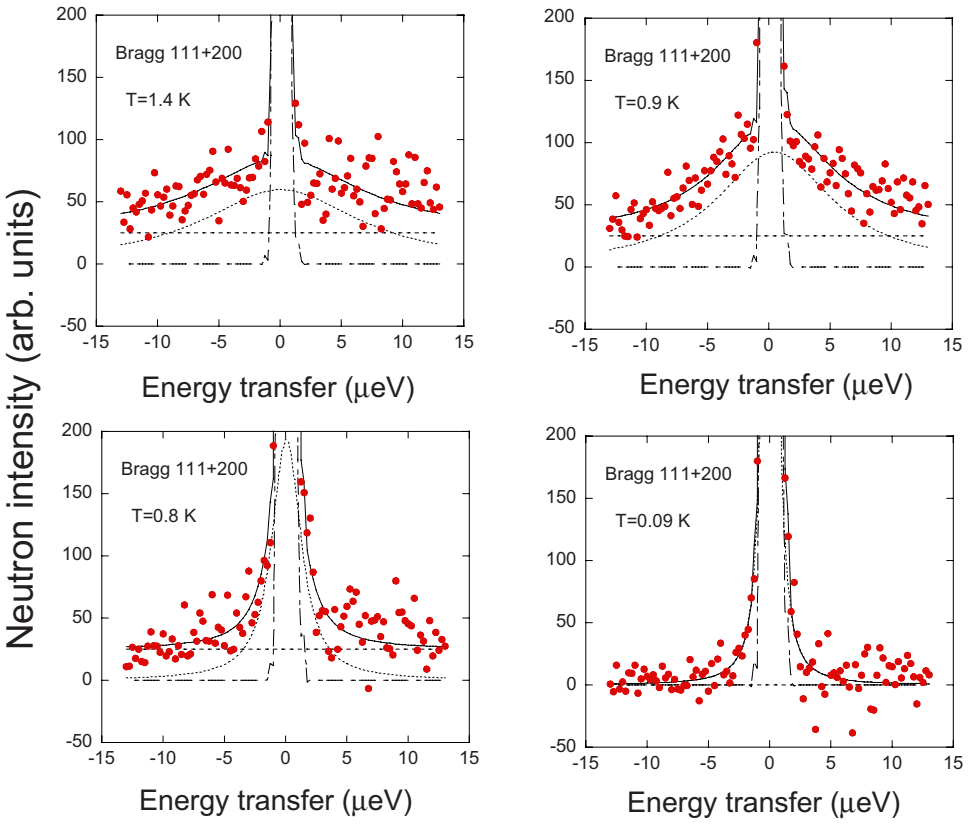

FIG. 3. (Color online) Inelastic neutron spectra of $Tb_2Sn_2O_7$ for several temperatures measured in the Q range of the 111 and 200 Bragg peaks. The solid line is a fit as described in the text. Dotted, dashed-dotted, and dashed lines correspond to the quasielastic, elastic, and flat background terms, respectively.

the accessible Q range. We have situated these Q bands in the diffraction pattern of Fig. 2. One sees that the Bragg Q bands mostly probe the long length scales (the Bragg intensity dominates), whereas the low, medium, and high Q bands probe the shortest length scale. We also note that the nuclear Bragg contribution on all of the above peaks is either zero or negligible and that the overall nuclear incoherent contribution is also small due to the small incoherent cross sections of the elements. By fitting the vanadium patterns with a Gaussian function, we get an energy resolution at HWHM of 0.4 μeV in the Bragg peak and large-angle regions, and 0.55 μeV in the low-angle region.

Typical energy-resolved neutron-scattering patterns are shown in Fig. 3 in the Q band covering the 111 and 200 Bragg peaks. They clearly show a quasielastic signal in the temperature range of 0.8–1.2 K. The quasielastic signal strongly narrows with decreasing temperature, which reflects the freezing of the spin dynamics around the transition. The neutron intensity was fitted by the sum of three contributions. First, an elastic (or resolution-limited) signal of intensity C_1 of mostly magnetic origin, which accounts for the spins which fluctuate at time scales longer than the resolution limit. Second, a Lorentzian function of intensity C_2 and HWHM Γ accounts for the quasielastic signal. The Lorentzian quasielastic signal was convoluted by the instrumental resolution. An energy-independent flat level "background" C_B accounts for the "fast" fluctuations (or short-time scales), corresponding to energy widths larger than the energy window. Above 1 K, the flat level and the rather broad Lorentzian contributions cannot be determined independently with good accuracy. So, the value of C_B was fixed to the value at 0.9 K. Below 0.6 K, the quasielastic linewidth has the same order of magnitude as the resolution, and the flat level vanishes.

The parameters deduced from the fits were plotted versus temperature in Fig. 4 in the Q band of the 111 and 200 Bragg peaks. Similar results were obtained for the Q band of the 220 peak. The elastic intensity C_1 increases with decreasing T. Its temperature variation scales quite well with that of the Bragg intensity deduced from diffraction data. The latter represents a constant angle integral of the scattering cross section over energy transfers up to the incident neutron energy (inset of Fig. 4). Just below T_C=0.87(2) K, the intensity measured by diffraction increases more sharply with decreasing T than the elastic intensity. The differences in the T dependence of the Bragg peak and the elastic resolved intensities can be explained by two factors: one being the possibility of integrating the fast dynamics (represented by the flat level in the energy-resolved experiment) and the other being the coarser Q resolution of the time-resolved patterns, which integrate a contribution from the SRO that is not included in the Bragg peaks of the diffraction patterns.

The quasielastic intensity C_2 shows a broad maximum in the transition region, where the contribution from the fast fluctuations starts to enter the energy window. As T decreases further, C_2 starts to decrease when the spectral weight is transferred to the elastic intensity. The energy width 2Γ decreases rapidly down to 0.8 K; a quasielastic signal of width close to the resolution limit remains at 0.09 K. The energy-independent flat level C_B also decreases with decreasing temperature. At 0.09 K, there is no visible contribution of the fast fluctuations to the energy pattern and C_B was fixed to zero.

The temperature variations of the parameters C_1, C_2, C_B, and Γ reflect a freezing of the spin dynamics. The elastic

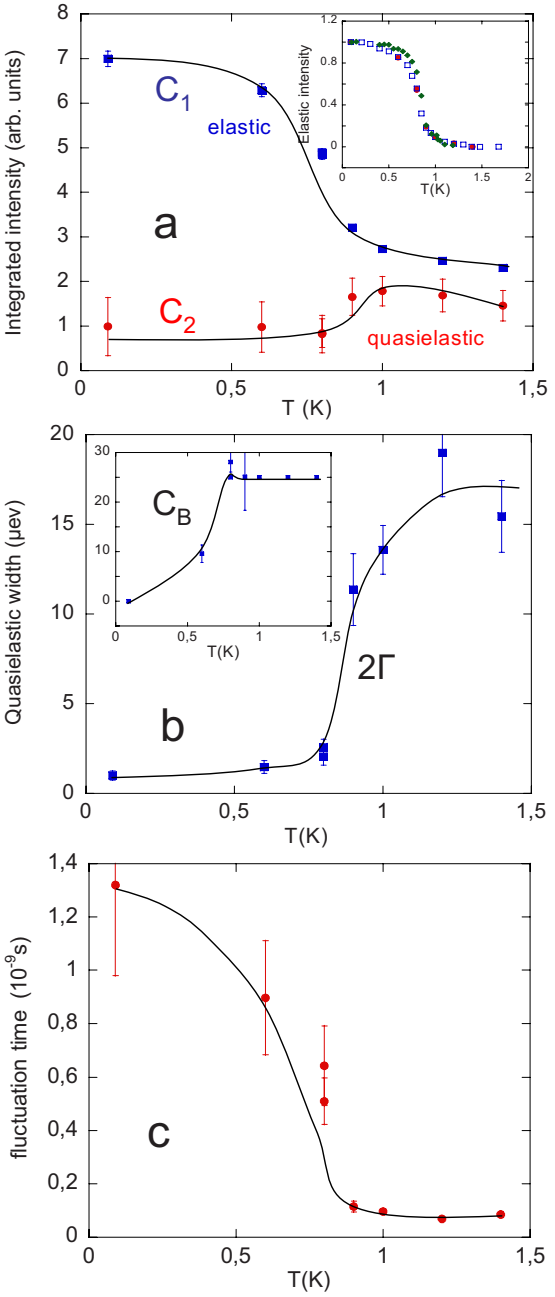

FIG. 4. (Color online) Temperature dependence of the parameters deduced from the fit of the inelastic spectra in the region of the 111 and 200 Bragg peaks. (a) Elastic intensity C_1 and quasielastic intensity C_2 deduced from the fit of the energy patterns. In the inset: the elastic intensity (full dots) is compared to the intensity from elastic scans (open squares) and to the integrated intensity of a magnetic Bragg peak measured in diffraction (diamonds). All quantities are scaled to vary between 1 at 0.1 K and 0 at 1.4 K. (b) Quasielastic width 2Γ versus temperature. In the inset: the background level C_B, involving fluctuations at a shorter time scale than probed in the energy window. (c) The fluctuation time $\tau=\hbar/\Gamma$. Solid lines are guides to the eye.

contribution increases at the expense of the fast fluctuations and quasielastic contributions, whereas the decrease of the linewidth reflects the increase of the relaxation time probed in the time window of the measurement.

The Lorentzian line shape of the quasielastic signal corresponds to a relaxation process which involves spin fluctuations with a lifetime τ ($\langle S(0)S(t)\rangle \propto e^{-t/\tau}$). Taking the Fourier transform of this expression yields $\tau=\hbar/\Gamma$, where $\hbar=0.658\times10^{-9}$ μeV s (see Ref. 15). The T dependence of the relaxation time is shown in Fig. 4(c). At 0.09 K, the time scale of the spin fluctuations is equal to $\tau_0=1.3\times10^{-9}$ s ($\Gamma=0.5$ μeV).

Energy spectra in the low, medium, and high Q bands also probe a freezing of the spin dynamics. Here, no contribution of a flat level was detected and the fits were performed with C_1 and C_2 contributions only. Their variations (Fig. 5) reflect those at the magnetic Bragg peaks. The Γ values at 0.09 K are higher, probing fluctuations at shorter time scales ($\tau_0\sim0.3-1\times10^{-9}$ s). The relative weight of the "fluctuating" spins with respect to the "static" spins at low temperature is also higher in the Q bands outside the Bragg peaks. Here the terms static and fluctuating refer to the time scale defined by the instrumental resolution of IN16 (1.3×10^{-9} s) and sensitivity of the fit.

One notices that due to the limited time window and the strong change of the correlations with temperature, the opposite variations of the quasielastic and elastic intensities during the freezing process do not compensate in a given Q band. Namely, at the Bragg peaks, the "loss" in the quasielastic intensity with decreasing temperature is much smaller than the "gain" in the elastic intensity, whereas the reverse situation occurs outside the Bragg peaks.

IV. DISCUSSION

The above features show a distribution of time scales, which extends to longer times with decreasing temperature, as the characteristic length scales of the spin correlations increase. Somewhat similar effects are seen in other frustrated magnets. A distribution of fluctuation times concomitant with a distribution of correlation lengths is observed by neutron scattering in disordered systems such as spin glasses.[16,17] A broad range of time scales in absence of long-range order but with remarkably energy(time)-scale invariant short-ranged correlations was also seen[18] in the well-known geometrically frustrated Kagome bilayer spin system $SrCr_{9x}Ga_{12-9x}O_{19}$ (SCGO).

The time scale of the fluctuations is in rather good agreement with the time scale probed by NSE experiment[12] in the range of the transition ($\tau\sim0.2\times10^{-9}$ s for $T=0.8$ K and $Q=0.08$ Å^{-1}). At 0.1 K, when NSE did not observe further dynamics, our experiment in the backscattering geometry still suggests fluctuations with time scales τ ranging from 0.3×10^{-9} to 1.3×10^{-9} s, the shortest time scale corresponding to the SRO. Fluctuations at longer time scales (above 1.3×10^{-9} s) do exist since they give rise to the elastic scattering and to a static response in the NSE experiment but no faster fluctuations are probed (there is no residual background in the energy window).

The range of the neutron derived characteristic times of the spin fluctuations must be compared with that probed by μSR experiments.[9,10] Indeed, the fluctuations with time scales longer than 1.3×10^{-9} s do not yield any static com-

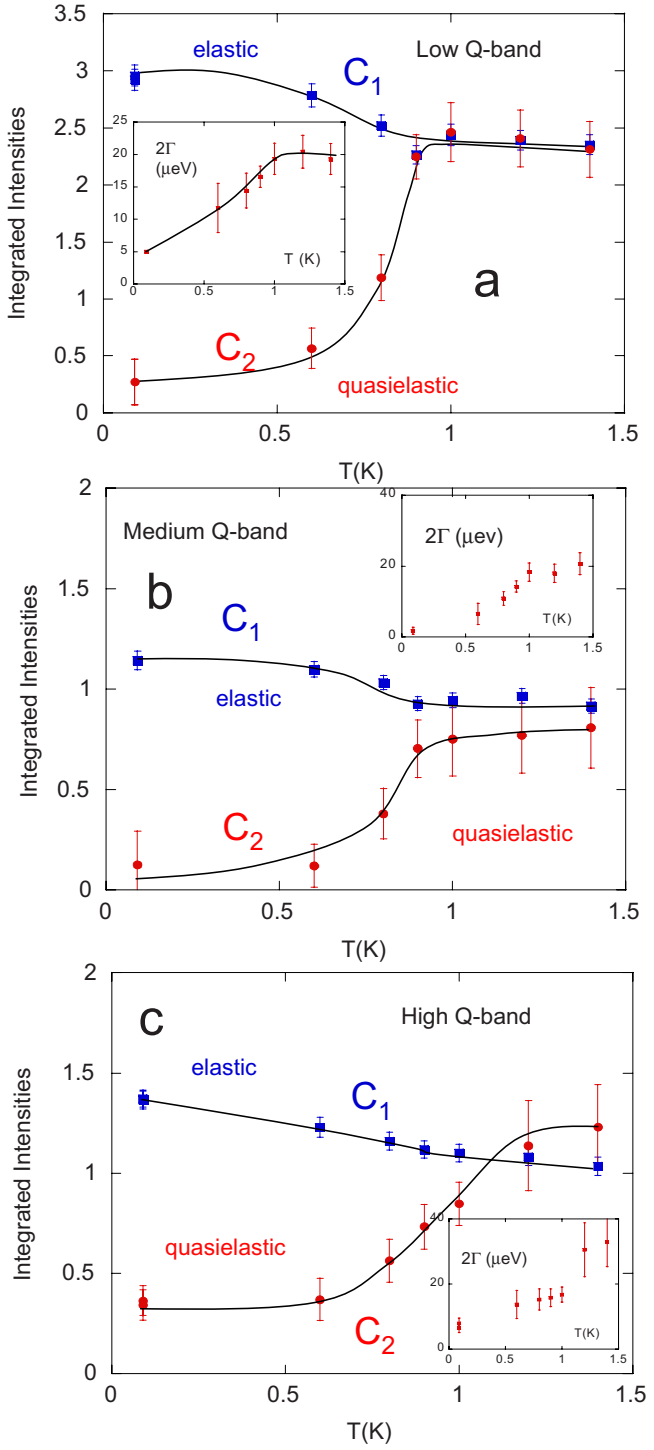

FIG. 5. (Color online) Temperature dependence of the integrated elastic and quasielastic intensities. The background level was fixed to zero at all temperatures. Solid lines are guides to the eye. (a)–(c) correspond to low, medium, and high Q bands, respectively. In the insets: the quasielastic width 2Γ versus temperature. The width at 0.09 K in the inset of (a) was fixed.

ponent in the muon spectra, where an exponential decay is observed above and below T_C=0.87 K. A strong fully static component cannot be excluded by the neutron data but seems to be incompatible with the muon results. In order to get a more quantitative insight for the comparison, we computed

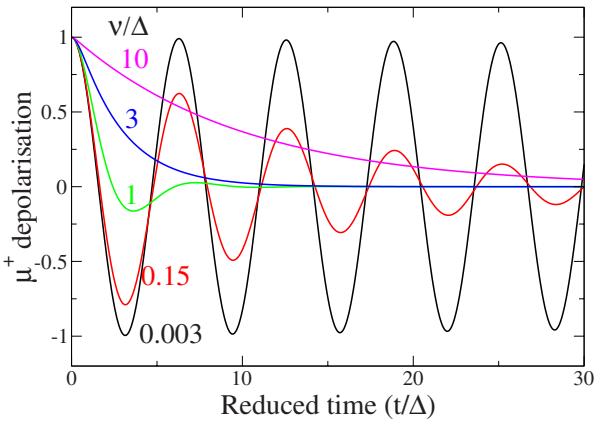

FIG. 6. (Color online) Positive muon depolarization function in the case of a dipolar field fluctuating perpendicular to the initial direction of polarization, for different values of the ratio ν/Δ (see text).

the longitudinal muon depolarization $P_Z(t)$ where the Z axis is the initial direction of the μ^+ polarization) in the presence of a (dipolar) field $B_{\rm loc}$ fluctuating randomly in time with a frequency ν. We used the stochastic theory developed, for instance, in Ref. 19, which assumes that the field jumps have a stationary and Markovian character. For the very simple case of a field perpendicular to the Z axis, the static depolarization function is merely $P_Z^{(0)}(t)=\cos\Delta t$, where $\Delta=\gamma_\mu B_{\rm loc}$, γ_μ=851.6 Mrad s^{-1} T^{-1} being the muon gyromagnetic ratio. Then, in terms of Laplace transforms, the dynamic depolarization is given by the standard expression in stochastic theory:[19]

$$P_Z(s)=\frac{P_Z^{(0)}(s+\nu)}{1-\nu P_Z^{(0)}(s+\nu)}=\frac{s+\nu}{\Delta^2+s\nu+s^2}. \qquad (1)$$

Integrating back to the time domain, the dynamical depolarization is obtained as a damped oscillation in the slow relaxation regime ($\nu<2\Delta$):

$$P_Z(t)=\exp\left(-\frac{\nu}{2}t\right)\left(\cos r\Delta t+\frac{\nu}{2r\Delta}\sin r\Delta t\right), \qquad (2)$$

where $r=\sqrt{1-\frac{\nu^2}{4\Delta^2}}$. The effect of the fluctuation is thus to reduce the pulsation by a factor r and to shift the phase of the oscillation by an angle φ such that $\tan\varphi=\frac{\nu}{2r\Delta}$. In the limiting case $\nu=2\Delta$, one gets $P_Z(t)=\exp(-\frac{\nu}{2}t)(1+\frac{\nu}{2}t)$, and in the fast relaxation regime ($\nu>2\Delta$) an expression analogous to Eq. (2) holds, with the trigonometric functions replaced by hyperbolic ones, and with $r=\sqrt{\frac{\nu^2}{4\Delta^2}-1}$. In this case, a damped decay is obtained, and in the extreme narrowing limit ($\nu\gg\Delta$), a true exponential decay occurs: $P_Z(t)=\exp(-\lambda_Z t)$, with $\lambda_Z=\frac{\Delta^2}{\nu}$; hence the expression for the μSR derived characteristic time $\tau_\mu=1/\nu=\lambda_Z/\Delta^2$.

The behavior of the dynamic depolarization function is sketched in Fig. 6 for different values of the ratio ν/Δ. The method of Ref. 19 can be used to deal with more complex spin fluctuations, such as in plane or along six directions, for instance. But for our purposes, we restrict ourselves to transverse fluctuations. To our knowledge, the dynamical depolar-

ization (2) has not been used in the past or has been observed experimentally but we think it could be relevant to spin fluctuations in the magnetically ordered phase of frustrated systems, where the μ^+ is submitted to a single fluctuating dipolar field. We believe that this situation occurs in $Tb_2Sn_2O_7$, when the local field arises from well correlated spins which fluctuate as a whole.

The above considerations show that fluctuations with a time scale τ_μ shorter than $\tau_l = 1/(2\gamma_\mu B_{\mathrm{loc}})$ should wash out the precession signal, which is the clear-cut signature of a static field in the muon data. In the μSR works, the exponential time decay was interpreted by a relaxation process between different configurations of the local field B_{loc}. At 0.1 K, $\lambda_Z \simeq 2.3\ \mu s^{-1}$ and the characteristic time scale, evaluated using the above relation for τ_μ, depends on the estimation of the otherwise unknown Δ or B_{loc} value; τ_μ is found to be 8×10^{-11} s in Ref. 9, assuming $B_{\mathrm{loc}}=0.2$ T, and 5×10^{-9} s in Ref. 10, assuming $B_{\mathrm{loc}}=0.02$ T. The former value (with $B_{\mathrm{loc}}=0.2$ T) is below the range estimated from the inelastic neutron data ($0.3-1.3\times10^{-9}$ s) but the latter is compatible with the presence of elastic scattering. Actually, given the measured λ_Z value at 0.1 K, one can obtain on the one hand the minimum value of the local field compatible with the absence of oscillating μSR signal: $\tau_\mu = \lambda_Z/\Delta^2 < \tau_l = 1/(2\Delta)$, yielding $B_{\mathrm{loc}} > 2\lambda_Z/\gamma_\mu$, i.e., $B_{\mathrm{loc}} > 5.4$ mT. On the other hand, the lower time limit yields an upper value for B_{loc}: $\tau_\mu > 0.3\times10^{-9}$ s yields $B_{\mathrm{loc}} < 0.1$ T. Comparison between muon and neutron data therefore favors a lower estimation of the internal field.

The mechanism leading to cooperative fluctuations of well correlated spins, as observed in ordered $Tb_2Sn_2O_7$ and $Gd_2Sn_2O_7$ pyrochlores,[9,10,20] remains to be understood. The fluctuations of the local field in $Tb_2Sn_2O_7$ are similar to those in $Tb_2Ti_2O_7$ spin liquid. Moreover in $Tb_2Ti_2O_7$, magnetic long-range ordered structures akin to ordered spin ice are stabilized by an applied field.[21] So one could speculate that in both cases the fluctuations of the local field involve tunneling or thermally activated excitations between the six degenerated configurations of the local spin ice structure.[10] In $Tb_2Sn_2O_7$, such excitations may help to "switch" domains of longer length scales. They could coexist/compete with standard spin waves within the ordered spin ice state.

In the $Tb_2Sn_2O_7$ ground state, we have probed by neutrons multiple length scales for the spin correlations. They might be connected with different spin components and time scales with no need to consider spatially independent clusters of different sizes. Together with the fluctuating field probed by muons, these features suggest very peculiar spin excitations in the ordered spin ice ground state. In geometrically frustrated magnets, only few calculations of the spin excitations have been done up to now. String modes of hexagonally bound clusters were predicted in pyrochlore spinels due to magnetoelastic effects.[22] Hexagonal clusters may account for the inelastic neutron scattering in $ZnCr_2O_4$ and $CdCr_2O_4$ pyrochlore spinels.[23,24] Such picture was also considered in spin ices, taking into account that spins on the pyrochlore lattice can be grouped into nonoverlapping hexagons without breaking the ice rules. However, in $Dy_2Ti_2O_7$ spin ice, recent work showed that the clusterlike scattering does not necessarily imply real independent hexagons.[25] On the other hand, in Kagome antiferromagnets, recent calculations of the dynamical structure factor predicted propagating excitations, with a strongly reduced spectral weight, down to very low temperatures.[26] It would be interesting to extend them to the pyrochlore lattice.

V. CONCLUSION

In conclusion, in $Tb_2Sn_2O_7$ ordered spin ice, we have observed a freezing of the spin fluctuations which involves the coexistence of different correlation lengths and times scales. The distribution extends to longer times with decreasing temperature. A marked slowing down is observed in the transition region, in agreement with previous muon and neutron spin-echo experiments. At the lowest temperature, the time scale of the spin fluctuations ranges between 1.3×10^{-9} and 0.3×10^{-9} s. Fluctuations at longer time scales are also observed by neutrons, whereas they give no clear-cut signature in the muon spectra. This may be compatible with the low estimation of the local field ($B_{\mathrm{loc}}=0.02$ T) found in μSR. The peculiar nature of the spin excitations probed in the ground state of the ordered spin ice remains to be explained by theory.

ACKNOWLEDGMENTS

We thank B. Frick and R. Chung for helping with the back scattering neutron experiment, O. Isnard for helping with the neutron-diffraction experiment, and J.-L. Ragazzoni for setting up the dilution equipment.

[1] A. P. Ramirez, A. Hayashi, R. J. Cava, R. Siddhartan, and B. S. Shastry, Nature (London) **399**, 333 (1999).
[2] J. Snyder, J. S. Slusky, R. J. Cava, and P. Schiffer, Nature (London) **413**, 48 (2001).
[3] S. T. Bramwell, M. J. Harris, B. C. den Hertog, M. J. P. Gingras, J. S. Gardner, D. F. McMorrow, A. R. Wildes, A. Cornelius, J. D. M. Champion, R. G. Melko, and T. Fennell, Phys. Rev. Lett. **87**, 047205 (2001).
[4] S. T. Bramwell and M. J. P. Gingras, Science **294**, 1495 (2001).
[5] H. Fukazawa, R. G. Melko, R. Higashinaka, Y. Maeno, and M. J. P. Gingras, Phys. Rev. B **65**, 054410 (2002).
[6] L. D. C. Jaubert, J. T. Chalker, P. C. W. Holdsworth, and R. Moessner, Phys. Rev. Lett. **100**, 067207 (2008).
[7] C. Castelnovo, R. Moessner, and S. L. Sondhi, Nature (London) **451**, 42 (2008).
[8] I. Mirebeau, A. Apetrei, J. Rodriguez-Carvajal, P. Bonville, A. Forget, D. Colson, V. Glazkov, J. P. Sanchez, O. Isnard, and E. Suard, Phys. Rev. Lett. **94**, 246402 (2005).
[9] P. Dalmas de Réotier, A. Yaouanc, L. Keller, A. Cervellino, B. Roessli, C. Baines, A. Forget, C. Vaju, P. C. M. Gubbens, A.

Amato, and P. J. C. King, Phys. Rev. Lett. **96**, 127202 (2006).
[10] F. Bert, P. Mendels, A. Olariu, N. Blanchard, G. Collin, A. Amato, C. Baines, and A. D. Hillier, Phys. Rev. Lett. **97**, 117203 (2006).
[11] I. Mirebeau, P. Bonville, and M. Hennion, Phys. Rev. B **76**, 184436 (2007).
[12] Y. Chapuis, A. Yaouanc, P. Dalmas de Réotier, S. Pouget, P. Fouquet, A. Cervellino, and A. Forget, J. Phys.: Condens. Matter **19**, 446206 (2007).
[13] K. C. Rule, G. Ehlers, J. R. Stewart, A. L. Cornelius, P. P. Deen, Y. Qiu, C. R. Wiebe, J. A. Janik, H. D. Zhou, D. Antonio, B. W. Woytko, J. P. Ruff, H. A. Dabkowska, B. D. Gaulin, and J. S. Gardner, Phys. Rev. B **76**, 212405 (2007).
[14] O. G. Randl, ILL Report No. 96RA07T, 1996 (unpublished).
[15] This expression for the typical time scale holds because it results from an energy measurement and a Fourier transform. This is the case for quasielastic or inelastic neutron scattering, electronic paramagnetic resonance, Mössbauer spectroscopy, or energy-resolved nuclear magnetic resonance (NMR). The characteristic time is obtained from a dynamical broadening or from the overall fluctuation line shape associated with the physical process so that it is the inverse of a pulsation ω, namely, $\tau = 1/\omega = 1/(2\pi\nu)$, where ν is the frequency equivalent to the energy $\hbar\omega$ involved in the process. On the reverse, when the typical time scale is determined from a time measurement such as muon spectroscopy or time-resolved NMR, where the measured quantity decays as $e^{-t/\tau}$, then $\tau = 1/\nu$ is the inverse of a frequency. This is also the case when τ is simply defined with respect to the frequency of a physical event as being the average time between two events.
[16] A. P. Murani, J. Phys. F: Met. Phys. **15**, 417 (1985).
[17] C. Bellouard, M. Hennion, I. Mirebeau, and B. Hennion, J. Magn. Magn. Mater. **104-107**, 1627 (1992).
[18] C. Mondelli, H. Mutka, B. Frick, and C. Payen, Physica B: Condensed Matter **266**, 104 (1999); H. Mutka, G. Ehlers, C. Payen, D. Bono, J. R. Stewart, P. Fouquet, P. Mendels, J. Y. Mevellec, N. Blanchard, and G. Collin, Phys. Rev. Lett. **97**, 047203 (2006).
[19] S. K. Dattagupta, Hyperfine Interact. **11**, 77 (1981).
[20] E. Bertin, P. Bonville, J.-P. Bouchaud, J. A. Hodges, J. P. Sanchez, and P. Vulliet, Eur. Phys. J. B **27**, 347 (2002).
[21] H. Cao, A. Gukasov, I. Mirebeau, P. Bonville, and G. Dhalenne, Phys. Rev. Lett. **101**, 196402 (2008).
[22] O. Tchernyshyov, R. Moessner, and S. L. Sondhi, Phys. Rev. Lett. **88**, 067203 (2002).
[23] S.-H. Lee, C. Broholm, W. Ratcliff, G. Gasparovic, Q. Huang, T. H. Kim, and S.-W. Cheong, Nature (London) **418**, 856 (2002).
[24] K. Kamazawa, S. Park, S.-H. Lee, T. J. Sato, and Y. Tsunoda, Phys. Rev. B **70**, 024418 (2004).
[25] T. Yavors'kii, T. Fennell, M. J. P. Gingras, and S. T. Bramwell, Phys. Rev. Lett. **101**, 037204 (2008).
[26] J. Robert, B. Canals, V. Simonet, and R. Ballou, Phys. Rev. Lett. **101**, 117207 (2008).